Successive bioanode regenerations to maintain efficient current production from biowaste

A. Bridier [a,1], E. Desmond-Le Quemener [a,1], C. Bureau [a], P. Champigneux [a], L. Renvoise [b], J.-M. Audic [b], E. Blanchet [c], A. Bergel [c], T. Bouchez [a,*]

[a] IRSTEA, URHBAN, centre d'Antony, 92761 Antony, France
[b] Suez Environnement — CIRSEE, 38, rue du président Wilson, 78230 Le Pecq, France
[c] Laboratoire de Génie Chimique (LGC), CNRS, Université de Toulouse (INPT), 4 allée Emile Monso, 31432 Toulouse, France

Keywords:
Microbial fuel cell
Bioanode
Biowaste
Biofilm
Electroactive

A B S T R A C T

The long term operation of efficient bioanodes supplied with waste derived organics is a key challenge for using bioelectrochemical systems as a waste valorization technology. Here, we describe a simple procedure that allowed maintaining highly efficient bioanodes supplied with biowaste. Current densities up to 14.8 A/m^2 were obtained with more than 40% of the electrons introduced as biowaste being recovered in the electrical cir cuit. Three fed batch reactors were started at different biowaste loading rates. A decline of coulombic efficiencies between 22 and 31% was recorded depending on the reactor over the first 3 weeks of operation. A renewal pro cedure of the anode was thereafter implemented, which led to a recovery of initial performances. The second and the third renewal, allowed maintaining stable high level performances with coulombic efficiency of approxi mately 40% over at least 3 weeks. Electroactive biofilm dynamics were monitored using 16S rRNA gene amplicon sequencing. Retrieved sequences were dominated by *Geobacter sulfurreducens* related reads (37% of total se quences), which proportion however varied along the experiment. Interestingly, sequences affiliated to various Bacteroidetes groups were also abundant, suggesting an adaptation of the anodic biofilm to the degradation of biowaste through metabolic interactions between microbial community members.

1. Introduction

Microbial fuel cells (MFCs) take advantages of the ability of microor ganisms to catalyze the oxidation of organic and inorganic matter and transfer extracted electrons to an electrode leading to the generation of current [1]. Electricity can thus be generated from a variety of pure compounds especially volatile fatty acids (VFAs) but also, and more interestingly, from complex organic matter mixtures such as wastes, ex pediently coupling the remediation process with the valorization of the reducing potential contained in waste [2,3]. Wastewaters [4 11] or solid activated sludges [12 15] were indeed successfully used for the produc tion of electric current in MFCs. Wang et al. [16] evaluated for instance the bioelectricity power production from two different sewage sludges in a MFC and reported a maximum power of 38.1 W·m^{-3} for an anaero bic activated sludge.

Bio wastes represent another potentially interesting resource of reduc ing power at the anode for bioelectrochemical systems. Indeed these wastes coming from biodegradable garden and park wastes, food wastes from households, restaurants, caterers and retail premises or comparable wastes from food processing plants [17] are abundant and highly rich in organic molecules. The amount of bio wastes available each year in France is estimated at 22.1 million tons [18]. Focusing on food wastes, a re cent FAO report showed that more than 1.3 billion tons per year of food globally produced for human consumption is lost before reaching the con sumer, thus constituting a huge amount of unused resources [19,20]. Fac ing this enormous potential, bio waste valorization constitutes therefore a major challenge for the development of a more sustainable world.

An open question for the utilization of such complex organic sub strates in bioelectrochemical systems is the achievable performances. Lower power is generally obtained when fermentable substrates are present, which have to be catabolized through multiple metabolic steps before being used by electroactive bacteria, as shown in experi ments using glucose as a substrate [21 23]. Freguia et al. indeed showed that glucose is used by fermentative bacteria, producing mainly hydro gen and acetate which can further be used for bacterial electricity gen eration [24]. A wide variety of metabolic pathways involving different microbial groups and their interaction can thus be engaged due to the diversity of substrates available in bio wastes. The heterogeneity of bio waste composition and the potential complexity of bacterial inter actions therefore require a careful examination of the conditions allowing the sustainable operation of bioelectrochemical systems

* Corresponding author at: 1 rue Pierre-Gilles de Gennes CS10030, 92761 Antony cedex, France.
E-mail address: theodore.bouchez@irstea.fr (T. Bouchez).
[1] These authors contributed equally to the work.

http://dx.doi.org/10.1016/j.bioelechem.2015.05.007

supplied with this complex feedstock [25]. In this respect, we analyzed three fed batch bioelectrochemical systems supplied with different loadings of biowaste. An operation strategy which consisted in a bioanode renewal procedure was implemented in order to optimize re actor performances and durability. The evolution of bioelectrocatalytic performances was monitored using a 3 electrode chemical setup to avoid rate limitations not related to bioanode kinetics [26]. In parallel, detailed microbial dynamics were determined using high throughput 16S rRNA gene amplicon sequencing analysis over a two month exper imental period.

2. Materials and methods

2.1. Biowaste preparation

Reconstituted biowastes were produced in a reproducible way to mimic the mean composition of food wastes from supermarkets and water was added to obtain a biowaste with 10% dry mass. They were composed of (percentages in mass) potatoes (8.1%), tomatoes (3.4%), beef patty (8.1%), milk powder (0.7%), biscuits (4.1%), and water (75.6%) and stored for 7 days at 35 °C in 1 L bottles for fermentation. The biowaste was then centrifuged and the supernatant sampled and frozen at −20 °C. The final pH was 3.9 and soluble COD 63 g/L. The com position revealed using ion chromatography (cf. below) was (g COD/L): butyric acid (9.7), propionic acid (1.9), lactic acid (11.2), acetic acid (0.4), and others (proteins, sugars, other organic acids, lipids) (39.8).

2.2. Configuration and operation of bioelectrochemical reactors

Bioelectrochemical reactors consisted of custom H cells with two 1.5 L glass chambers separated by a cation exchange membrane (CEM) (Fumasep® FKE, Germany) and sealed together with a clamping ring. Anodic and cathodic compartments were filled with 1 L of Bio chemical Methane Potential (BMP) medium (NF EN ISO 11734) buffered with carbonates (8 g HCO_3^-/L). The anode was a 4 cm × 4 cm piece of carbon cloth (Paxitech®, France) connected to the external cir cuit by a platinum wire (Heraeus®, 0.5 mm) pushed through a thick butyl rubber stopper inserted in the bottle cap. The cathode was a 4 cm × 4 cm stainless steel plate (Outokumpu®, 254 SMO, Germany) screwed on a stainless steel shaft (DURAN® DU.1200386) bent into a J shape. Three reactors were operated at 35 °C under N_2 atmosphere and with a pH regulation at 7 using an automated NaOH (0.1 mol/L) ad dition system in anodic compartments. Anodic compartments were connected to gas tight plastic bags (Cloup, France) which allowed keep ing the pressure at the atmospheric level and collecting the gas pro duced. The cathodic compartment was continuously sparged with CO_2 to remove the hydrogen produced and avoid its diffusion to the anodic compartment. These three reactors were supplied with different con centrations of biowastes for each reactor by injecting different volumes of the biowaste solution made as mentioned previously.

The anode was used as a working electrode in a 3 electrode setup. A saturated calomel electrode (SCE, +0.24 V vs. Standard Hydrogen Elec trode, SHE) was used as a reference electrode in the anodic compart ment. Chronoamperometries were performed for the three reactors using a multi channel potentiostat (BioLogic®, France, VMP3, EC Lab software) with anode potential poised at +0.16 V vs. SCE (+0.40 V vs. SHE) and measurements of mean currents every 15 min. Coulombic efficiency was obtained by calculating the ratio of total recovered cou lombs by integrating the current over time to the theoretical amount of coulombs that could be produced from biowastes for each feeding phase (cf. Fig. 1) (Equation 1):

$$CE \quad \frac{M_{O_2} \int_{t_1}^{t_2} I(t)dt}{F \; b \; N \; m_{COD}}$$

where M_{O_2} is the molecular weight of oxygen, I the intensity, t_1 and t_2 times corresponding respectively to the beginning and the end of the feeding phase, F Faraday's constant, b = 4 the number of mole of elec trons exchanged per mole of oxygen, N the number of substrate injec tions for the feeding phase and m_{COD} the introduced mass of COD for each injection (m_{COD} = 63, 126 and 189 mg COD for R1, R2 and R3 re spectively from day 0 to day 41, m_{COD} = 252 and 315 mg COD for R2 and R3 respectively from day 41 to day 55). Since COD concentrations were not measured in the reactor, it is possible that incomplete oxida tion of the COD introduced accounted for part of the apparent e loss measured by this CE calculation.

Interestingly, the CE calculated this way can be reformulated as the ratio between the valorization rate R_v and the supply rate R_s both expressed in g COD/m^2/day: CE = R_v / R_s with (Equation 2 and Equation 3)

$$R_v \quad \frac{M_{O_2} \int_{t_1}^{t_2} I(t)dt}{F \; b \; (t_2 - t_1) \; S}$$

$$R_s \quad \frac{N \; m_{COD}}{(t_2 - t_1) \; S}$$

where S is the surface of the electrode.

2.3. Bioanode development and renewal procedures

An activated sludge sampled in a wastewater treatment plant (Achères, France) was used as an inoculum for the primary bioanode formation. A first run was thus started in the bioelectrochemical reactor after the addition of 600 mg/L acetate in the anodic compartment con taining activated sludges (10% *v*/*v*) and with anode potential poised at +0.16 V vs. SCE (+0.40 V vs. SHE). A second run was then successively performed by injecting 20 mL of biowastes at 63 g COD/L as the sub strate. The resulting bioanode was used as a primary anode in our work by connecting a 1 cm × 1 cm fragment of this primary anode de veloped on acetate and biowastes to the platinum wire with a clean 4 cm × 4 cm carbon cloth as adapted from Liu et al. [27]. At different ex periment times, anodes were renewed according to a similar procedure. Briefly, the carbon cloth anode was removed from the reactors and a fragment of 1 cm × 1 cm of this anode was attached to a new 4 cm × 4 cm clean carbon cloth anode. Both fragments were then con nected together in close contact to the platinum wire, introduced in the reactor in a clean medium and used as a new anode. The remaining piece of the old anode was stored at −20 °C for microscopic and molecular analyses.

2.4. Chemical analyses

Before each daily feeding event, a sample was recovered from the anodic compartment and analyzed. VFA concentrations were measured using ion chromatography (DIONEX DX 120, column IONPAC® ICE AS1 (9 × 250 mm)).The mobile phases were heptafluorobutyric acid (0.4 mmol/L) and TBAOH (5 mmol/L). Acetate, propionate, butyrate, lactate, formate and valerate acids can be quantified from 10 mg/L to 500 mg/L.

Gas composition was determined using gas chromatography (Varian CP 4900). The three columns mounted on this device enabled the quan tification of O_2, N_2, CH_4, CO_2, H_2, H_2S, and NO_2.

2.5. Microbial analyses

2.5.1. Molecular microbial community analysis

Carbon cloth electrodes were removed from MFCs at different times during the course of the experiment and cells were recovered by scratching and vortexing electrodes in a 150 mM NaCl sterile solution

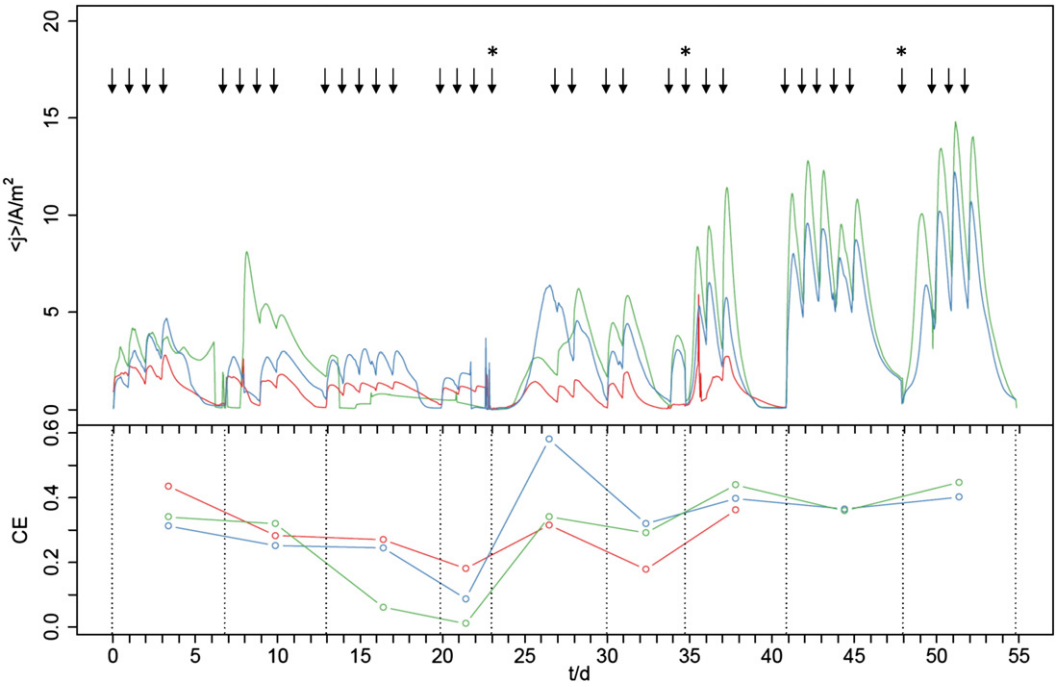

Fig. 1. Chronoamperometry and anodic coulombic efficiency for the three reactors. (Top) Current density plotted against time for the reactors 1 (red), 2 (blue) and 3 (green) supplied respectively with biowaste at loading rates of 63, 126 (or 252 after day 41) and 189 (or 315 after day 41) mg COD per injection. Arrows represent the different biowaste injections in the anodic compartment and stars indicate renewal of the anode. (Bottom) Coulombic efficiencies (CEs) for the different feeding phases are figured in the bottom of the picture and calculated with respect to introduced COD. Feeding phases are delimited by dotted lines and lasted for one week, except when electrode renewal occurred.

and then by centrifugating the resulting suspension. Total DNA was extracted from the pellet using the Powersoil™ DNA isolation kit (MoBio laboratories) according to the manufacturer's instructions. DNA concentrations were quantified using a quantifying fluorescent dye assay (Qubit dsDNA BR assay kits) and Qubit 2.0 Fluorometer (Invitrogen, Life Technologies). The V4 regions of the 16S SSU rDNA gene were then amplified using the archaeal/bacterial primers 515F (5′ GTGCCAGCMGCCGCGGTAA 3′) and 806R (5′ GGACTACHVGGGTWTCTAAT 3′) [28] (Eurofins) and Platinum® Pfx DNA polymerase (Invitrogen, Life Technologies). Fusion primers are constructed according to the recommendations of the protocol "Ion Amplicon Library Preparation (Fusion Method)." The sequences of barcodes are identical to those of "Ion Xpress™ Barcode Adapters 1 96 Kit", which allows direct recognition of barcodes by the PGM sequencer. The PCR reaction was performed using a Mastercycler Pro S thermocycler (Eppendorf) according to the following PCR conditions: 94 °C for 5 min, followed by 30 cycles of 94 °C for 15 s, 53 °C for 30 s and 68 °C for 1 min, and a final elongation step at 68 °C for 5 min. The PCR products were then controlled by agarose gel electrophoresis and purified using the Agencourt AMPure XP bead kit (Beckman Coulter) according to the "Ion Amplicon Library Preparation (Fusion Method)". Resulting libraries were then quantified using Agilent Bioanalyzer 2100 and the DNA 1000 kit (Agilent) according to manufacturer's instructions. Libraries were then diluted to 26 pM before being mixed in the same tube to be used for template preparation. The template was prepared with the Ion OneTouch2 using the Ion PGM Template OT2 400 kit (Ion torrent) according to the manufacturer's instructions. Amplicons carried by the ion sphere particles (ISP) prepared during the template preparation step were sequenced according to the "Ion PGM HI Q Sequencing" protocol using a 316V2 chip and the Ion Torrent PGM™ platform (Ion Torrent, life technologies) at the IRSTEA MIMOSE platform (Antony, France).

Resulting data were analyzed with the open source software package QIIME "Quantitative Insights Into Microbial Ecology" [29]: 16S DNA sequence quality was controlled using a sliding window of 50 nt long requiring an average quality above 25. The sequences were thus trimmed to the end of the last window with required average quality and discarded if their final length was less than 150 nt. In addition, the remaining reads where the longest homopolymer was greater than 6 nt or containing an ambiguous base were also discarded. Sequences were then aligned with PyNAST [30] using the Silva 108 database core aligned set formatted for QIIME as a template [31]. Putative chimeric sequences were identified with ChimeraSlayer [32] and removed from the dataset. The remaining sequences were clustered in operational taxonomic units (OTUs) at 97% sequence similarity using uclust [33]. OTU assignment was then performed with the RDP classifier [34,35] a 0.8 bootstrap cut off using the most abundant sequence in each OTU as a representative sequence.

Representative sequences of major OTUs were introduced in the ARB software [36] to check the quality of taxonomic assignations and infer bacterial species when possible.

2.5.2. Biofilm imaging

Biofilms formed on electrodes were visualized at different time of development by confocal laser scanning microscopy (Zeiss LSM 510) and a 40× oil immersion lens. Prior to imaging, total cells of electrode biofilm were stained using the Syto9® fluorescent marker according to the manufacturer instruction (Molecular Probes, Invitrogen, USA). Images were obtained using an excitation wavelength of 488 nm and a BP500 530 emission filter for Syto9 fluorescence. Carbon cloth fibers were also visualized using reflection imaging with a 543 nm laser.

3. Results and discussion

3.1. Electrochemical performances

Three reactors R1, R2 and R3 were operated simultaneously and supplied with different loadings of biowaste at the anodic compartment. The electrochemical performances obtained are shown in Fig. 1 which

displays the current density and coulombic efficiency over time for the three reactors.

The operation consisted of two phases: a first phase, from day 0 to day 41, where the three reactors R1, R2 and R3 were supplied with biowaste at loading rates of 63, 126 and 189 mg COD per injection respectively, and a second phase, from day 41 to day 55, where R2 and R3 were operated at higher loading rates of 252 mg COD and 315 mg COD, respectively while R1 was stopped. Results confirmed the possibility to produce current using biowaste as the substrate at the anode. Indeed, for the three reactors we observed that each biowaste injection (figured by arrows) leads to a current density peak. We did not observed a direct proportionality between the amount of biowaste introduced and the level of current density peaks in the three reactors. However, maximal current densities of 2.8, 6.5 and 11.4 A/m^2 were respectively reached for R1, R2 and R3 in the first phase and illustrate that the highest biowaste concentration was associated with the highest current density. The current densities measured here are higher than what was previously obtained in similar experimental conditions with a 3 electrode setup and real effluents. Cercado Quezada et al. report 1.5 and 1.6 A/m^2 maximal current density on carbon felt bioanodes fed with dairy wastes (792 ± 131 mg/L and 272 mg/L COD [37,38]. It is also higher than the maximal 6.4 A/m^2 obtained by Ketep et al. [39] in continuous feeding with pulp and paper mill effluent on smooth graphite plates (406 mg COD/day). In the latter case, however, the difference in current density may be explained by the difference in the active electrode surface. Indeed the surface available for microbial colonization is greater on our carbon cloth than on smooth graphite plates.

The mean coulombic efficiencies (CEs) were calculated for every biowaste feeding phase which are figured at the bottom of Fig. 1 by vertical dotted lines. It corresponds to the ratio between total electrons flowing in the circuit during the feeding phase and electrons available as extrapolated from total introduced COD measurements. It should be noted that the COD introduced at the anode under the form of biowaste is not necessarily totally biodegradable, and it led here to an underestimation of the CE in comparison to those classically calculated using consumed COD [39].

On the first week, CE was comprised between 31 and 44% depending on reactors. Since VFAs constitute 37% of the total COD of the biowaste and that they were totally consumed after one day as revealed by chemical analyses (data not shown), it suggests that VFAs could be used as the main source of electrons in the anodic compartment.

Between day 0 and day 23, CE continuously decreased in the three reactors and fell at values ranging from 1 to 18% depending on the reactor considered. As methane production is frequently reported in MFC reactors and lead to a severe decrease of CE [40 42], measurement of gas composition in the anodic compartment was undertaken. It revealed that CH_4 production was limited (CH_4 concentrations never exceeding 1%) and stable during this period showing that this progressive loss of efficiency was not due to a development of methanogenic archaeal populations. Another possible explanation for the progressive CE decrease could be linked to the aging of the anodic biofilm. Indeed, the emergence of chemical gradients due to the increase of biofilm thickness could impact the physiological state of resident cells and their ability to transfer electrons. In agreement with this, Renslow et al. demonstrated that the conductivity of a *Geobacter sulfurreducens* biofilm decreases beyond a thickness of 170 μm. The consequent decline in the current density recorded was due to the limitation of substrate diffusion and also the increase of resistivity of the thick biofilm [43]. Virdis et al. [44] also showed that an aged biofilm with high thickness (>100 μm) can be characterized by diminished electrocatalytic current densities due to the fact that cytochromes in this biofilm were mainly in the reduced redox state. However, they observed this phenomenon only in *G. sulfurreducens* pure culture biofilms after 80 days and not in old mixed culture biofilms suggesting that the strategies adopted by mixed biofilms and *Geobacter* pure culture biofilms to control electron flow cannot be directly compared.

In order to thwart this decrease of performances, a fraction of the colonized electrode was replaced by clean carbon cloth poised at the same potential at day 23 (see Materials and methods). Interestingly, this renewal procedure (figured by stars in Fig. 1) led to an increase of electrochemical performances of the three reactors as revealed by the coulombic efficiency curves. Indeed, CE rose at similar levels to those observed at t_0 for R1 and R3 and even reached 58% for R2. CE augmentation was also observable after the anode renewal at day 35 showing the reproducibility of this phenomenon. These observations are supported by previous studies showing better electrochemical performance of MFCs for which anode was inoculated using the biofilm harvested from the anode of an existing MFC [27,45 48]. For instance, Liu et al. [27] developed a procedure to increase the bioelectrochemical activity of an acetate fed anodic biofilm which consists in using a primary biofilm formed from wastewater to inoculate directly a new clean graphite electrode to develop a secondary biofilm. They showed that the bioelectrocatalytic current density of a MFC can be doubled from 250 μA/cm^2 to 500 μA/cm^2 between the primary and the secondary anodic biofilm. Similarly, using layered corrugated carbon as anode material, Baudler et al. [48] reported that the bioelectrocatalytic activity of secondary biofilms is about two times higher (6.7 mA/cm^2) than that of primary biofilms (3 mA/cm^2). In our case, the procedure was used to start the BES leading to high current densities and coulombic efficiencies, and then repeated three times in the course of the experiment leading to a restoration of the initial performance level for all the newly formed bioanodes. Our results therefore demonstrate that, in addition to a successful strategy for MFC start up, the renewal procedure could also be used several times to maintain the efficiency of the bioanode during its operation. Moreover, we show that this procedure can be effective not only on acetate but also on complex substrates such as biowaste, which constitutes a first step towards its industrial implementation.

At day 41, the increase of biowaste injections to 252 mg or 315 mg COD in R2 and R3 respectively was correlated with an increase of current density (max: 12.2 and 14.8 A/m^2) in both reactors, particularly

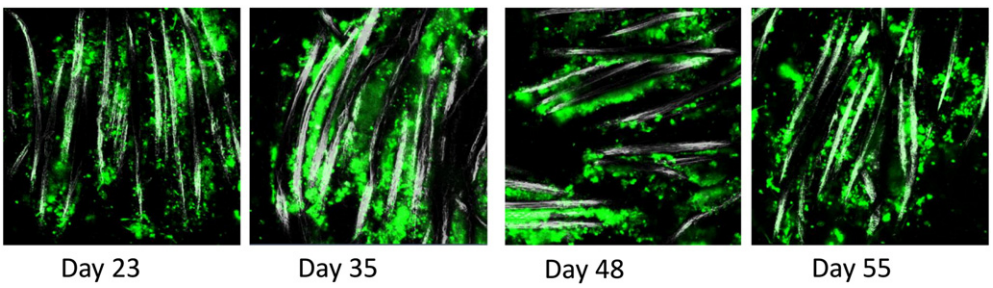

Fig. 2. Biofilm imaging. Confocal images of anodic biofilms. Biofilm morphology was examined using CLSM and Syto9® fluorescent dyeing at days 23, 35, 48 and 55. Results are shown for the reactor 2 as representative illustrations of the three reactors because they exhibited similar anodic colonization. Pictures display the bacterial cells in green and the carbon cloth fibers in white. Scale bars correspond to 50 μm.

in R2. A slight decrease of coulombic efficiency was nevertheless observed concomitantly to this increase of current densities but the anode renewal at day 48 again led to a slight increase of the coulombic efficiency with stabilization around 40%, a slightly higher value than those observed at the beginning of the experiment. The highest COD valorization rate obtained in our system was measured during these last feeding phases in R3. It reached 51.5 g COD/m^2/day for the last phase with a supply rate of 115.2 g COD/m^2/day, resulting in a CE of 44.7% (Fig. 1). However, if the maximal valorization rate of our system would have been reached, an increase of the supply rate would have led to a decrease of the CE. The stable CE values recorded at different loading rates therefore suggest that we did not reach the saturation of the biofilm oxidation capacity. The performances of our bioanodes still appeared relatively high in comparison with those obtained in the same kind of systems with 3 electrodes and supplied with complex substrates. Ketep et al. [39] reported for instance a maximal CE of 25% from consumed COD in a 3 electrode set up supplied with paper mill effluent. Working on dairy wastes, Cercado Quezada et al. [37] obtained a maximal CE of 42% from introduced COD with an anode formed from garden compost. However, in this last study, maximal current density reached 3.5 A/m^2 whereas we obtained here maximal current densities of 12.2 and 14.8 A/m^2 for R2 and R3 respectively that correspond to a better COD valorization rate. The renewal procedure applied in our bioelectrochemical systems supplied with biowastes therefore allowed maintaining a high level of bioelectrocatalytic performance over a prolonged period. The obtained maximal valorization rate around 50 g COD/m^2/day is interesting in the perspective of using this kind of system as a waste valorization technology. Indeed, when considering a surface to volume ratio of 40 m^2/m^3 as reported for carbon cloth in large bioelectrochemical reactors [49] the valorization rate would be 2 kg COD/m^3/day, which corresponds to medium to high volumetric rates commonly encountered in wastewater treatment plants [50].

3.2. Microbial community analysis

Confocal observations clearly revealed an important colonization of carbon cloth for days 23, 35, 48, 55. Microbes were in close association with carbon cloth fibers and irregularly covered the carbon cloth surface. However, these observations did not reveal marked differences when comparing different time points for the three reactors in terms of anodic bacterial colonization as shown in Fig. 2 for reactor 2 given as an illustrative representation.

The microbial communities of the three reactors were examined throughout the experiment using PGM Ion Torrent 16S rDNA amplicon sequencing by targeting the V4 region. The number of reads obtained ranged from 9449 to 33,831 for the different samples with mean length between 189 bp and 261 bp. A total of 716 operational taxonomic units (OTUs) were obtained after bioinformatics analysis.

The Shannon index (H) and Simpson's index of diversity (1 − D) calculated for the microbial communities of our bioanodes (Tables 1 and 2) were low in comparison with diversity indexes measured for environmental microbial ecosystems found in soils (Shannon index from 4.74 to 5.99) [39] or wastewaters (Shannon index from 6.26 to 7.36 and evenness index from 0.77 to 0.92) [40], but, as underlined by Dennis et al. [53], it was expected given the strong selective pressure found in our systems. Both diversity indexes appeared similar when comparing days 23, 48 and 55 for the three reactors (from 4.1 to 4.9 for the Shannon index and from 0.83 to 0.89 for Simpson's index of diversity), while they were lower on day 35 (from 1.7 to 2.5 for the Shannon index and from 0.38 to 0.55 for Simpson's index of diversity). It indicates that a high selection occurred in the three reactors after the first electrode renewal but that microbial diversity recovered its original level with the next two renewals. More precisely, Simpson's index of diversity measures the evenness of the different microbial populations, thus the very low scores measured at day 35 revealed that the corresponding biofilms are dominated by few species.

Table 1
Shannon diversity indexes. Shannon diversity indexes (H) obtained considering 16S rDNA sequences retrieved from electroactive biofilm samples for R1, R2 and R3 during the course of experiment.

	Day 23	Day 35	Day 48	Day 55
R1	4.42	2.51	NA	NA
R2	4.19	1.70	4.38	4.90
R3	4.40	1.83	4.10	4.45

Temporal evolution of the proportions of major orders (representing at least 1% of the sequences on at least one electrode) identified are shown in Fig. 3.

Six of them numbered more than 10% of sequences on at least one of the electrodes: Bacteroidales (Bacteroidetes), Clostridiales (Firmicutes), Desulfuromonadales (Proteobacteria), Pseudomonadales (Proteobacteria), Spirochaetales (Spirochaetes) and an unidentified order affiliated to Bacteroidetes. Except for Spirochaetes the bacterial phyla found here (Bacteroidetes, Firmicutes and Proteobacteria) have been repeatedly identified on bioanodes [42, 51 54]. After the first 23 days of operation, the three biofilms sampled were dominated by three different orders: Desulfuromonadales for reactor 1, unidentified Bacteroidetes for reactor 2 and Bacteroidales for reactor 3. At day 35, 12 days after the first electrode renewal, all three biofilms were highly dominated by Desulfuromonadales which explains the low diversity indexes measured above. At days 48 and 55, after the next two electrode renewals, microbial populations were more balanced, either dominated by Desulfuromonadales or Bacteroidales.

To identify the main species dominating our biofilms, we investigated with the ARB software [36] the phylogeny of OTUs accounting for more than 1% of total sequences. The relative abundances of those species are shown in Fig. 4.

G. sulfurreducens was the major species identified, and it accounts for 37% of all sequences analyzed in our study. It is a well known electroactive microorganism able to oxidize H_2, acetate, formate and lactate with an electrode as the terminal electron acceptor [55]. It was thus probably directly involved in the oxidation of lactate (17.8% of total COD) and acetate (0.6% of total COD) found in our biowastes and in electron exchange at the anode. It, however, doesn't explain alone the high percentage of COD recovered in the circuit as electrons (CE up to 58%) observed during the different feeding phases (Fig. 1). The second main species identified *Proteiniphilum acetatigenes*, a proteolytic Bacteroidetes [56] was accounting for 17% of total sequences. It was first isolated from tricultures degrading propionate to acetate together with *Syntrophobacter sulfatireducens* (a δ proteobacterium) and *Methanobacterium formicicum* [56]. It has been shown to produce acetic acid and propionic acid from proteinaceous material and might thus cooperate with *G. sulfurreducens* to produce electricity from complex substrates such as biowastes. Other Bacteroidetes found in our biofilms are *Petrimonas sulfuriphila*, uncultured Bacteroidales belonging to the Vadinbc27 wastewater sludge group and bacteria classified as Vc2.1 bac22. *P. sulfuriphila* is known to produce acetate from diverse carbohydrates [57] and might thus also provide acetate for *Geobacter* using complex substrates. The other Bacteroidales are commonly found in anaerobic digestion systems. As for sequences identified as Vc2.1

Table 2
Simpson's indexes of diversity. Simpson's indexes of diversity (1 D) obtained considering 16S rDNA sequences retrieved from electroactive biofilm samples for R1, R2 and R3 during the course of experiment.

	Day 23	Day 35	Day 48	Day 55
R1	0.86	0.55	NA	NA
R2	0.83	0.38	0.89	0.88
R3	0.87	0.42	0.84	0.88

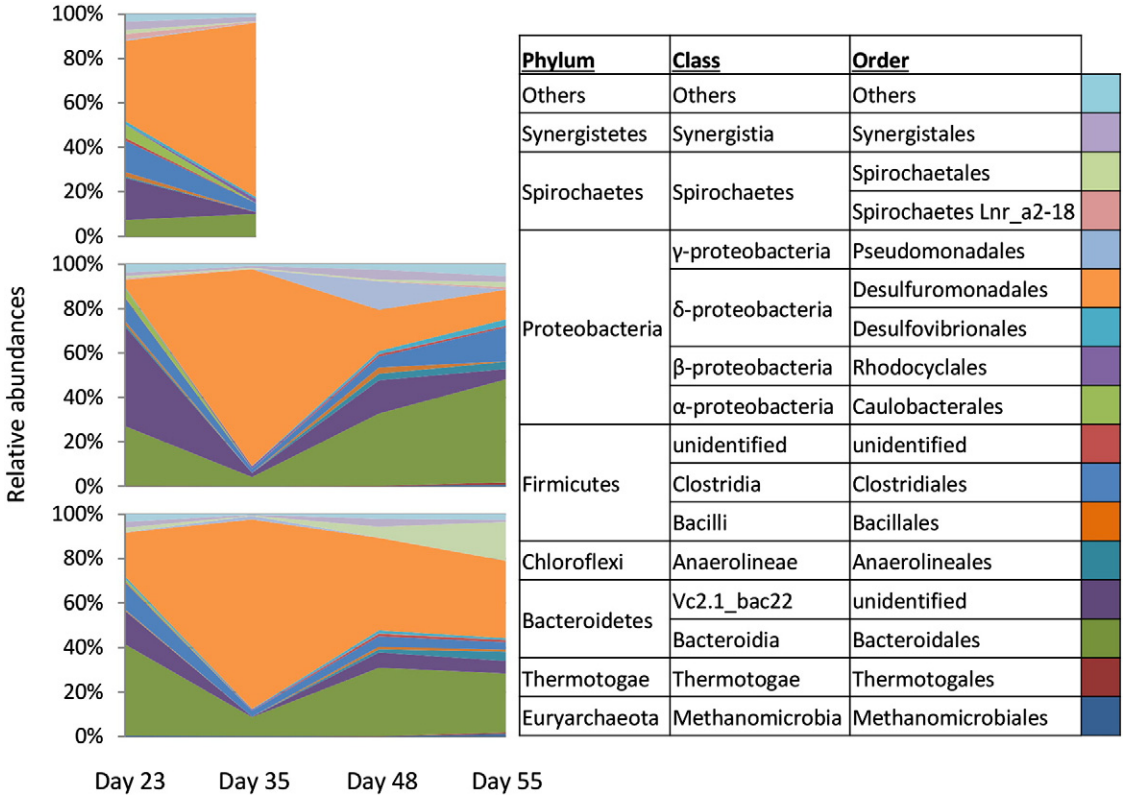

Phylum	Class	Order
Others	Others	Others
Synergistetes	Synergistia	Synergistales
Spirochaetes	Spirochaetes	Spirochaetales
		Spirochaetes Lnr_a2-18
Proteobacteria	γ-proteobacteria	Pseudomonadales
	δ-proteobacteria	Desulfuromonadales
		Desulfovibrionales
	β-proteobacteria	Rhodocyclales
	α-proteobacteria	Caulobacterales
Firmicutes	unidentified	unidentified
	Clostridia	Clostridiales
	Bacilli	Bacillales
Chloroflexi	Anaerolineae	Anaerolineales
Bacteroidetes	Vc2.1_bac22	unidentified
	Bacteroidia	Bacteroidales
Thermotogae	Thermotogae	Thermotogales
Euryarchaeota	Methanomicrobia	Methanomicrobiales

Fig. 3. Microbial diversity of anodic biofilms. Relative abundance of major taxonomic groups (order level) in the three reactors over time. Taxonomic assignment was performed with the RDP classifier as detailed previously. Taxa representing > 1% of assignable sequences in one or more samples are shown, while taxa present in < 1% of sequences in all samples are grouped in the 'Others' category.

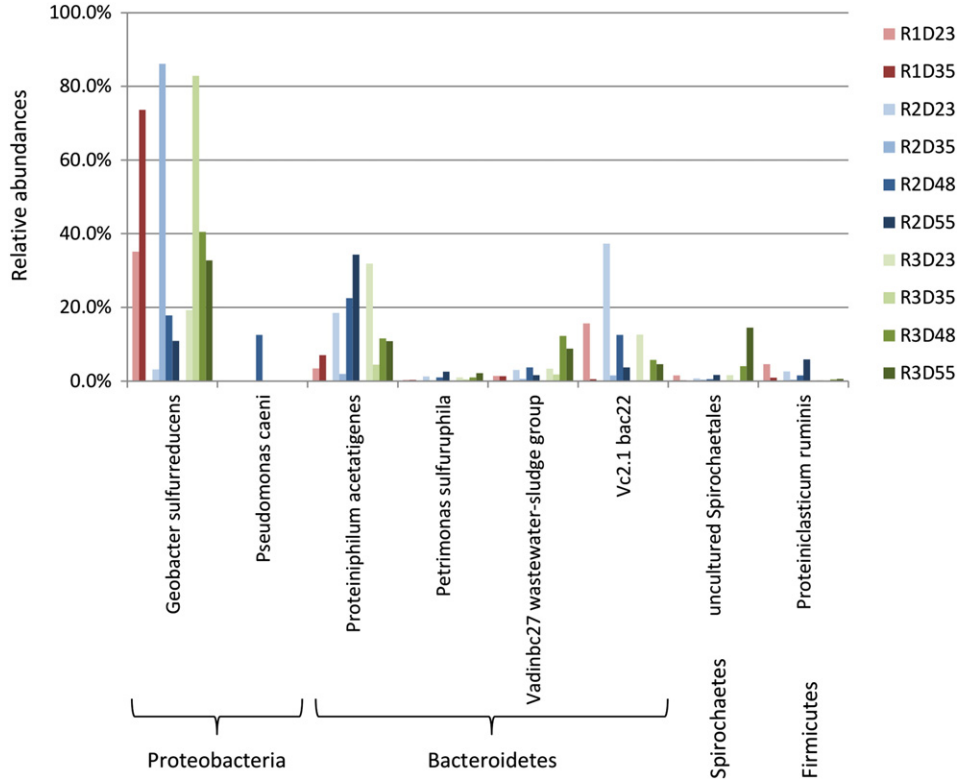

Fig. 4. Relative abundance of main species. Bar charts of the eight species corresponding to the eleven OTUs accounting for more than 1% of total sequences. They include altogether 75% of total sequences. Species identified from reactor 1 at days 23 and 35 are shown in blue color scale and denoted as R1D23 and R1D35. Species identified from reactor 2 at days 23, 35, 48 and 55 are shown in red color scale and denoted as R2D23, R2D35, R2D48 and R2D55. Species identified from reactor 3 at days 23, 35, 48 and 55 are shown in green color scale and denoted as R3D23, R3D35, R3D48 and R3D55. Bacterial phyla are indicated in the bottom.

bac22, they accounted for 9% of total sequences and thus constituted the third major OTU, they were mainly present at day 23 constituting the major class identified on electrode 2, but their role is mysterious since the most closely related sequence was only identified as a minor component of a microbial population implicated in syntrophic degradation of limonene [58] and no cultured organism from the group is known. The last OTUs have been identified as uncultured Spirochaetales mainly found in R3, *Pseudomonas caeni* a denitrifying bacterium punctually found at day 48 in R2, and *Proteiniclasticum ruminis*.

An intriguing point of microbial population dynamics was the discrepancy in *Geobacter* proportions after the first renewal (70 to 90%) and after the next renewals (10 to 40%). Indeed, it doesn't seem to influence bioanode performances as CE values and current densities reached similar levels after each renewal. These results suggest that the development of a stable population degrading biowastes and transferring electrons to the anode, did not appear here to be directly related to the sole proportion of *G. sulfurreducens* on the anode but rather to the settlement of an association of different bacterial taxa including *Geobacter* with different Bacteroidales. Such association could enable an optimization of resource utilization throughout the ability to perform complementary metabolic pathways as mentioned previously. In line with this, the recent work showed that *G. sulfurreducens* can oxidize acetate in syntrophic association with a hydrogenotrophic exoelectrogen, *Hydrogenophaga* sp., with current generation. The authors demonstrated that current generation and acetate degradation were highest in the coculture than in the *G. sulfurreducens* pure culture [59]. Our results suggest that the anode renewal procedure allows a dynamic reorganization of the biofilm structure towards a more efficient electrocatalytic architecture, resulting from the availability of a clean carbon cloth surface. This should be investigated through dedicated microscopic studies.

4. Conclusion

In this contribution, we demonstrated that biowastes can be successfully used to supply a bioanode with potential poised at +0.4 V vs. SHE and produce bioelectricity with high current densities and high coulombic efficiencies. The maximal valorization rate obtained is interesting in the perspective of using this technology as an industrial waste valorization bioprocess. The microbial diversity observed on our bioanodes suggests the importance of metabolic interactions between community members for the optimal utilization of the complex cocktail of molecules contained in biowastes. Moreover the anode renewal procedure possibly introduces a blank electrode surface that allows a reorganization of the biofilm towards an optimization of the electron transfer from biowaste to the electrical circuit. In practice, this simple procedure appears as an efficient strategy to maintain a high level of bioelectrocatalytic performance over a prolonged period in bioelectrochemical systems supplied with a complex organic substrate such as biowaste.

Acknowledgments

This work has benefited from a support of the French state managed by the Agence Nationale de la Recherche, within the framework of the French Investissement d'Avenir program (project number ANR 10 BTBR 02).

References

[1] B.E. Logan, B. Hamelers, R.A. Rozendal, U. Schrorder, J. Keller, S. Freguia, P. Aelterman, W. Verstraete, K. Rabaey, Microbial fuel cells: methodology and technology, Environ. Sci. Technol. 40 (2006) 5181–5192.
[2] D. Pant, G. Van Bogaert, L. Diels, K. Vanbroekhoven, A review of the substrates used in microbial fuel cells (MFCs) for sustainable energy production, Bioresour. Technol. 101 (2010) 1533–1543.
[3] B.E. Logan, J.M. Regan, Electricity-producing bacterial communities in microbial fuel cells, Trends Microbiol. 14 (2006) 512–518.
[4] T. Shimoyama, S. Komukai, A. Yamazawa, Y. Ueno, B.E. Logan, K. Watanabe, Electricity generation from model organic wastewater in a cassette-electrode microbial fuel cell, Appl. Microbiol. Biotechnol. 80 (2008) 325–330.
[5] H. Liu, R. Ramnarayanan, B.E. Logan, Production of electricity during wastewater treatment using a single chamber microbial fuel cell, Environ. Sci. Technol. 38 (2004) 2281–2285.
[6] O. Lefebvre, Z. Tan, Y.J. Shen, H.Y. Ng, Optimization of a microbial fuel cell for wastewater treatment using recycled scrap metals as a cost-effective cathode material, Bioresour. Technol. 127 (2013) 158–164.
[7] S.V. Mohan, R. Saravanan, S.V. Raghavulu, G. Mohanakrishna, P.N. Sarma, Bioelectricity production from wastewater treatment in dual chambered microbial fuel cell (MFC) using selectively enriched mixed microlora: effect of catholyte, Bioresour. Technol. 99 (2008) 596–603.
[8] Z. He, S.D. Minteer, L.T. Angenent, Electricity generation from artificial wastewater using an upflow microbial fuel cell, Environ. Sci. Technol. 39 (2005) 5262–5267.
[9] P. Kaewkannetra, W. Chiwes, T.Y. Chiu, Treatment of cassava mill wastewater and production of electricity through microbial fuel cell technology, Fuel 90 (2011) 2746–2750.
[10] F. Kargi, S. Eker, Electricity generation with simultaneous wastewater treatment by a microbial fuel cell (MFC) with Cu and Cu–Au electrodes, J. Chem. Technol. Biotechnol. 82 (2007) 658–662.
[11] V.R. Nimje, C.Y. Chen, H.R. Chen, C.C. Chen, Y.M. Huang, M.J. Tseng, K.C. Cheng, Y.F. Chang, Comparative bioelectricity production from various wastewaters in microbial fuel cells using mixed cultures and a pure strain of *Shewanella oneidensis*, Bioresour. Technol. 104 (2012) 315–323.
[12] D. Suor, J.X. Ma, Z.W. Wang, Y.L. Li, J.X. Tang, Z.C. Wu, Enhanced power production from waste activated sludge in rotating-cathode microbial fuel cells: the effects of aquatic worm predation, Chem. Eng. J. 248 (2014) 415–421.
[13] Z.W. Wang, X.J. Mei, J.X. Ma, Z.C. Wu, Recent advances in microbial fuel cells integrated with sludge treatment, Chem. Eng. Technol. 35 (2012) 1733–1743.
[14] Z. Ge, F. Zhang, J. Grimaud, J. Hurst, Z. He, Long-term investigation of microbial fuel cells treating primary sludge or digested sludge, Bioresour. Technol. 136 (2013) 509–514.
[15] J. Jiang, Q. Zhao, J. Zhang, G. Zhang, D.J. Lee, Electricity generation from biotreatment of sewage sludge with microbial fuel cell, Bioresour. Technol. 100 (2009) 5808–5812.
[16] Z.W. Wang, J.X. Ma, Y.L. Xu, H.G. Yu, Z.C. Wu, Power production from different types of sewage sludge using microbial fuel cells: a comparative study with energetic and microbiological perspectives, J. Power Sources 235 (2013) 280–288.
[17] Directive_2008/98/EC, Directive_2008/98/EC of the European Parliament and of the council on waste and repealing certain directives, Off. J. Eur. Union L 312 (2008).
[18] ADEME, Réduire, trier et valoriser les biodéchets des gros producteurs, Ademe Report 2013, pp. 1–132.
[19] C.S.K. Lin, L.A. Pfaltzgraff, L. Herrero-Davila, E.B. Mubofu, S. Abderrahim, J.H. Clark, A.A. Koutinas, N. Kopsahelis, K. Stamatelatou, F. Dickson, S. Thankappan, Z. Mohamed, R. Brocklesby, R. Luque, Food waste as a valuable resource for the production of chemicals, materials and fuels. Current situation and global perspective, Energy Environ. Sci. 6 (2013) 426–464.
[20] J. Parfitt, M. Barthel, S. Macnaughton, Food waste within food supply chains: quantification and potential for change to 2050, Phil. Trans. R. Soc. B 365 (2010) 3065–3081.
[21] S. Jung, J.M. Regan, Comparison of anode bacterial communities and performance in microbial fuel cells with different electron donors, Appl. Microbiol. Biotechnol. 77 (2007) 393–402.
[22] S.B. Velasquez-Orta, E. Yu, K.P. Katuri, I.M. Head, T.P. Curtis, K. Scott, Evaluation of hydrolysis and fermentation rates in microbial fuel cells, Appl. Microbiol. Biotechnol. 90 (2011) 789–798.
[23] T.H. Yang, M.V. Coppi, D.R. Lovley, J. Sun, Metabolic response of Geobacter sulfurreducens towards electron donor/acceptor variation, Microb. Cell Factories 9 (2010).
[24] S. Freguia, K. Rabaey, Z.G. Yuan, J. Keller, Syntrophic processes drive the conversion of glucose in microbial fuel cell anodes, Environ. Sci. Technol. 42 (2008) 7937–7943.
[25] P.K. Barua, D. Deka, Electricity generation from biowaste based microbial fuel cells, International Journal of Energy, Information and Communications 1 (2010) 77–92.
[26] M. Rimboud, D. Pocaznoi, B. Erable, A. Bergel, Electroanalysis of microbial anodes for bioelectrochemical systems: basics, progress and perspectives, Phys. Chem. Chem. Phys. 16 (2014) 16349–16366.
[27] Y. Liu, F. Harnisch, K. Fricke, R. Sietmann, U. Schroder, Improvement of the anodic bioelectrocatalytic activity of mixed culture biofilms by a simple consecutive electrochemical selection procedure, Biosens. Bioelectron. 24 (2008) 1006–1011.
[28] J.G. Caporaso, C.L. Lauber, W.A. Walters, D. Berg-Lyons, C.A. Lozupone, P.J. Turnbaugh, N. Fierer, R. Knight, Global patterns of 16S rRNA diversity at a depth of millions of sequences per sample, Proc. Natl. Acad. Sci. U. S. A. 108 (2011) 4516–4522.
[29] J.G. Caporaso, J. Kuczynski, J. Stombaugh, K. Bittinger, F.D. Bushman, E.K. Costello, N. Fierer, A.G. Pena, J.K. Goodrich, J.I. Gordon, G.A. Huttley, S.T. Kelley, D. Knights, J.E. Koenig, R.E. Ley, C.A. Lozupone, D. McDonald, B.D. Muegge, M. Pirrung, J. Reeder, J.R. Sevinsky, P.J. Tumbaugh, W.A. Walters, J. Widmann, T. Yatsunenko, J. Zaneveld, R. Knight, QIIME allows analysis of high-throughput community sequencing data, Nat. Methods 7 (2010) 335–336.
[30] J.G. Caporaso, K. Bittinger, F.D. Bushman, T.Z. DeSantis, G.L. Andersen, R. Knight, PyNAST: a flexible tool for aligning sequences to a template alignment, Bioinformatics 26 (2010) 266–267.
[31] C. Quast, E. Pruesse, P. Yilmaz, J. Gerken, T. Schweer, P. Yarza, J. Peplies, F.O. Glockner, The SILVA ribosomal RNA gene database project: improved data processing and web-based tools, Nucleic Acids Res. 41 (2013) D590–D596.

[32] B.J. Haas, D. Gevers, A.M. Earl, M. Feldgarden, D.V. Ward, G. Giannoukos, D. Ciulla, D. Tabbaa, S.K. Highlander, E. Sodergren, B. Methe, T.Z. DeSantis, J.F. Petrosino, R. Knight, B.W. Birren, H.M. Consortium, Chimeric 16S rRNA sequence formation and detection in Sanger and 454-pyrosequenced PCR amplicons, Genome Res. 21 (2011) 494–504.
[33] R.C. Edgar, Search and clustering orders of magnitude faster than BLAST, Bioinformatics 26 (2010) 2460–2461.
[34] Q. Wang, G.M. Garrity, J.M. Tiedje, J.R. Cole, Naive Bayesian classifier for rapid assignment of rRNA sequences into the new bacterial taxonomy, Appl. Environ. Microbiol. 73 (2007) 5261–5267.
[35] J.R. Cole, Q. Wang, E. Cardenas, J. Fish, B. Chai, R.J. Farris, A.S. Kulam-Syed-Mohideen, D.M. McGarrell, T. Marsh, G.M. Garrity, J.M. Tiedje, The Ribosomal Database Project: improved alignments and new tools for rRNA analysis, Nucleic Acids Res. 37 (2009) D141–D145.
[36] W. Ludwig, O. Strunk, R. Westram, L. Richter, H. Meier, Yadhukumar, A. Buchner, T. Lai, S. Steppi, G. Jobb, W. Forster, I. Brettske, S. Gerber, A.W. Ginhart, O. Gross, S. Grumann, S. Hermann, R. Jost, A. Konig, T. Liss, R. Lussmann, M. May, B. Nonhoff, B. Reichel, R. Strehlow, A. Stamatakis, N. Stuckmann, A. Vilbig, M. Lenke, T. Ludwig, A. Bode, K.H. Schleifer, ARB: a software environment for sequence data, Nucleic Acids Res. 32 (2004) 1363–1371.
[37] B. Cercado-Quezada, M.L. Delia, A. Bergel, Treatment of dairy wastes with a microbial anode formed from garden compost, J. Appl. Electrochem. 40 (2010) 225–232.
[38] B. Cercado-Quezada, M.L. Delia, A. Bergel, Electrochemical micro-structuring of graphite felt electrodes for accelerated formation of electroactive biofilms on microbial anodes, Electrochem. Commun. 13 (2011) 440–443.
[39] S.F. Ketep, E. Fourest, A. Bergel, Experimental and theoretical characterization of microbial bioanodes formed in pulp and paper mill effluent in electrochemically controlled conditions, Bioresour. Technol. 149 (2013) 117–125.
[40] L. Zhuang, Q. Chen, S.G. Zhou, Y. Yuan, H.R. Yuan, Methanogenesis control using 2-bromoethanesulfonate for enhanced power recovery from sewage sludge in air-cathode microbial fuel cells, Int. J. Electrochem. Sci. 7 (2012) 6512–6523.
[41] K.J. Chae, M.J. Choi, K.Y. Kim, F.F. Ajayi, W. Park, C.W. Kim, I.S. Kim, Methanogenesis control by employing various environmental stress conditions in two-chambered microbial fuel cells, Bioresour. Technol. 101 (2010) 5350–5357.
[42] K.J. Chae, M.J. Choi, J.W. Lee, K.Y. Kim, I.S. Kim, Effect of different substrates on the performance, bacterial diversity, and bacterial viability in microbial fuel cells, Bioresour. Technol. 100 (2009) 3518–3525.
[43] R.S. Renslow, J.T. Babauta, A.C. Dohnalkova, M.I. Boyanov, K.M. Kemner, P.D. Majors, J.K. Fredrickson, H. Beyenal, Metabolic spatial variability in electrode-respiring *Geobacter sulfurreducens* biofilms, Energy Environ. Sci. 6 (2013) 1827–1836.
[44] B. Virdis, D. Millo, B.C. Donose, D.J. Batstone, Real-time measurements of the redox states of c-type cytochromes in electroactive biofilms: a confocal resonance raman microscopy study, PLoS One 9 (2014).
[45] K. Rabaey, G. Lissens, S.D. Siciliano, W. Verstraete, A microbial fuel cell capable of converting glucose to electricity at high rate and efficiency, Biotechnol. Lett. 25 (2003) 1531–1535.
[46] J.R. Kim, B. Min, B.E. Logan, Evaluation of procedures to acclimate a microbial fuel cell for electricity production, Appl. Microbiol. Biotechnol. 68 (2005) 23–30.
[47] E. Blanchet, B. Erable, A. Bergel, E. Desmond, A. Bridier, T. Bouchez, Improvement of Microbial Anode Performances for Treatment and Valorization of Organic Wastes, 10th European Symposium on Electrochemical Engineering, 2014.
[48] A. Baudler, S. Riedl, U. Schröder, Long-term performance of primary and secondary electroactive biofilms using layered corrugated carbon electrodes, Front. Energy Res. 2 (2014) 1–6.
[49] A. Janicek, Y. Fan, H. Liu, Design of microbial fuel cells for practical application: a review and analysis of scale-up studies, Biofuels 5 (2014) 79–92.
[50] Degrémont, Mémento technique de l'eau, Lavoisier (2005).
[51] S.X. Teng, Z.H. Tong, W.W. Li, S.G. Wang, G.P. Sheng, X.Y. Shi, X.W. Liu, H.Q. Yu, Electricity generation from mixed volatile fatty acids using microbial fuel cells, Appl. Microbiol. Biotechnol. 87 (2010) 2365–2372.
[52] J.W. Zhang, E.R. Zhang, K. Scott, J.G. Burgess, Enhanced electricity production by use of reconstituted artificial consortia of estuarine bacteria grown as biofilms, Environ. Sci. Technol. 46 (2012) 2984–2992.
[53] P.G. Dennis, K. Guo, M. Imelfort, P. Jensen, G.W. Tyson, K. Rabaey, Spatial uniformity of microbial diversity in a continuous bioelectrochemical system, Bioresour. Technol. 129 (2013) 599–605.
[54] S. Freguia, E.H. Teh, N. Boon, K.M. Leung, J. Keller, K. Rabaey, Microbial fuel cells operating on mixed fatty acids, Bioresour. Technol. 101 (2010) 1233–1238.
[55] A.M. Speers, G. Reguera, Electron donors supporting growth and electroactivity of *Geobacter sulfurreducens* anode biofilms, Appl. Environ. Microbiol. 78 (2012) 437–444.
[56] S.Y. Chen, X.Z. Dong, *Proteiniphilum acetatigenes* gen. nov., sp nov., from a UASB reactor treating brewery wastewater, Int. J. Syst. Evol. Microbiol. 55 (2005) 2257–2261.
[57] A. Grabowski, B.J. Tindall, V. Bardin, D. Blanchet, C. Jeanthon, *Petrimonas sulfuriphila* gen. nov., sp nov., a mesophilic fermentative bacterium isolated from a biodegraded oil reservoir, Int. J. Syst. Evol. Microbiol. 55 (2005) 1113–1121.
[58] A.E. Rotaru, R. Schauer, C. Probian, M. Mussmann, J. Harder, Visualization of candidate division OP3 cocci in limonene-degrading methanogenic cultures, J. Microbiol. Biotechnol. 22 (2012) 457–461.
[59] Z. Kimura, S. Okabe, Acetate oxidation by syntrophic association between *Geobacter sulfurreducens* and a hydrogen-utilizing exoelectrogen, ISME J. 7 (2013) 1472–1482.